

Detection and Separation of DNA and Silver Nanoparticles Using a Solid-State Nanopore

Bo Ding,[§] Xin-Yi Hong,[§] Han Yin, Jing-Yun Xu, Xiao-Yu Zhang, Qing Zhou, and Yang Shen*



Cite This: *ACS Omega* 2023, 8, 17682–17688

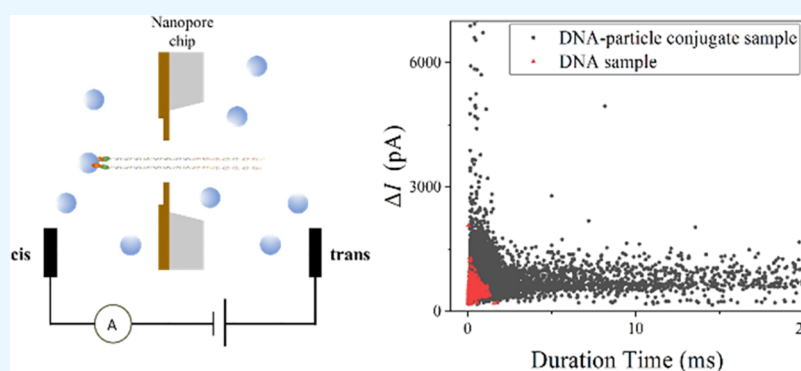


Read Online

ACCESS |

Metrics & More

Article Recommendations



ABSTRACT: Nanopore sensors, a new generation of single-molecule sensors, are increasingly used to detect and analyze various analytes and have great potential for rapid gene sequencing. However, there are still some problems in the preparation of small diameter nanopores, such as imprecise pore size and porous defects, while the detection accuracy of large-diameter nanopores is relatively low. Therefore, how to achieve more precise detection of large diameter nanopore sensors is an urgent problem to be studied. Here, SiN nanopore sensors were used to detect DNA molecules and silver nanoparticles (NPs) separately and in combination. The experimental results show that large-size solid-state nanopore sensors can identify and discriminate between DNA molecules, NPs, and NP-bound DNA molecules clearly according to resistive pulses. In addition, the detection mechanism of using NPs to assist in identifying target DNA molecules in this study is different from previous reports. We find that silver NPs can simultaneously bind to multiple probes and target DNA molecules and generate a larger blocking current than free DNA molecules when passing through the nanopore. In conclusion, our research indicates that large-sized nanopores can distinguish the translocation events, thereby identifying the presence of the target DNA molecules in the sample. This nanopore-sensing platform can produce rapid and accurate nucleic acid detection. Its application in medical diagnosis, gene therapy, virus identification, and many other fields is highly significant.

1. INTRODUCTION

Nanopore sensors, a new generation of single-molecule sensors, are increasingly used to detect and analyze various analytes, such as organic polymers, nanoparticles (NPs), proteins, and enzymes.^{1–4} Nanopore technology can analyze and identify individual molecules by measuring the modulation of ionic currents. The label-free method can capture hundreds of resistive pulse signals in a single second at a low cost and with high throughput. Moreover, the technique has great potential for rapid gene sequencing.

The nanopore sensor measures the modulation of ionic current caused by the analyte-induced physical blockage. Although pioneering research of this technology is based on protein nanopores, solid-state nanopores present obvious advantages over their biological counterparts, including high stability, controllable diameter and channel length, and variable adjustable surface properties. Thus, they could be integrated

into silicon-based devices and arrays. Besides, solid-state nanopores can adapt to various experimental conditions.¹ For example, in 2001, Li et al.⁵ succeeded in the detection of 500-bp double-stranded DNA (dsDNA) molecules by fabricating solid-state nanopores in a free-standing SiN membrane with a diameter of ~ 1.8 nm using an ion beam. Since then, technology has been the subject of extensive research and development over the past few decades. As a

Received: January 9, 2023

Accepted: April 27, 2023

Published: May 9, 2023



result, solid-state nanopores now have been used to detect the length, hybridization, and folding of DNA strands.

In recent years, several studies have demonstrated the creation of small nanopores; however, stabilizing the preparation of a solid-state nanopore with a diameter of less than 3 nm remains a formidable obstacle. TEM drilling can maintain pores smaller than 5 nm, but each nanopore requires a lengthy vacuum, making it inefficient. In addition, dielectric breakdown is commonly used to create tiny pores, but the size of the nanopores produced is imprecise, and it is simple to form porous defects. These difficulties in preparing nanopores with a small diameter led to the lack of repeatability of translocation current and the difficulty of corresponding analysis. For another, large pores have a low detection resolution, and it is challenging to distinguish nucleic acid molecules with different base sequences using the ionic current alone.

Recently, numerous alternative methods for DNA detection utilizing nanopores with a large diameter have been reported. For example, there have been studies in which the target DNA was selectively bound to a probe-coated bead to detect the target oligonucleotide.^{6,7} As the first successful attempt to use a solid-state nanopore as an ionic scanning device, Ling's team employed beads to slow DNA translocation when resolving individual hybridization segments (or "probes") on a DNA molecule, enabling standard patch-clamp electronics to detect DNA fragment signatures and DNA hybridization.^{8,9} Moreover, Booth et al.¹⁰ demonstrated a variable pressure method that can identify changes in particle surface charge using particle-by-particle analysis and resistive pulse sensing. This way, they can selectively detect and differentiate between "probe" and "target" bound beads. The results were validated using complementary techniques such as fluorescence and phase analysis light scattering. Schmidt's team^{11,12} proposed using PNA probes conjugated beads for sequence-specific DNA capture to charge neutral particles negatively, drive target beads electrically to the nanopore sensing zone, and generate a characteristic pulse ionic current. For instance, Zhang et al. demonstrated a sensitive and robust nanopore sensing scheme using highly specific γ -PNA probes conjugated beads to accurately detect miR-204 fragments against the small RNA background and analyze the duration of the resistive pulses.¹³ This study used the electro-osmotic flow as the driving force to move 0.97 μm beads through a 1 μm pore. The longer translocation time for the target beads confirms that electrophoretic force exerts the opposite effect on negatively charged particles, decreasing their electroosmotic velocity. Koo et al. also reported a similar phenomenon in their study.¹⁴ Furthermore, PNA probes with conjugated beads have also demonstrated great promise in the detection of microRNA,¹³ rRNA,¹⁵ and circular DNA¹⁶ targets with specific sequences. The studies above have achieved target DNA labeling and efficient detection by binding beads or probes to DNA molecules, indicating that the large nanopore sensor can also identify specific DNA molecules.

The detection of DNA molecules using the methods above, however, has some limitations due to the micron-sized diameter of the beads. There is a low probability that bead-bound DNA will pass through the nanopore, which results in a low DNA detection efficiency. NPs, a promising material for nucleic acid detection, are smaller in diameter than larger beads, making it easier for them to pass through the nanopore. Suppose the nanopore sensor can successfully detect and

differentiate between DNA molecules and NPs, it will be possible to detect nanoparticle-bound DNA molecules, and DNA detection efficiency is expected to increase.

In this study, SiN nanopore sensors were used to detect DNA molecules, silver NPs, and DNA molecules bound to NPs. We tried to demonstrate that nanopores with a large size can significantly differentiate the ionic current of NPs and DNA, thereby guiding NP-assisted detection of nucleic acid molecules.

2. MATERIALS AND METHODS

2.1. Nanopore Preparation. In order to prepare solid-state nanopore chips, nanopores must be integrated into the detection device using a cross-scale manufacturing strategy. Initially, the self-supported SiN membrane chip was fabricated using conventional semiconductor technology. The thickness of the SiN membrane deposited by low-pressure chemical vapor deposition (LPCVD) is 100 nm. At the center of the SiN membrane, a circular region of 2 μm in diameter was then thinned to 20 nm using a focused ion beam (FIB). Finally, a nanopore was drilled in the thinned region, and the nanopore's length is 20 nm. Figure 1A shows the scanning electron

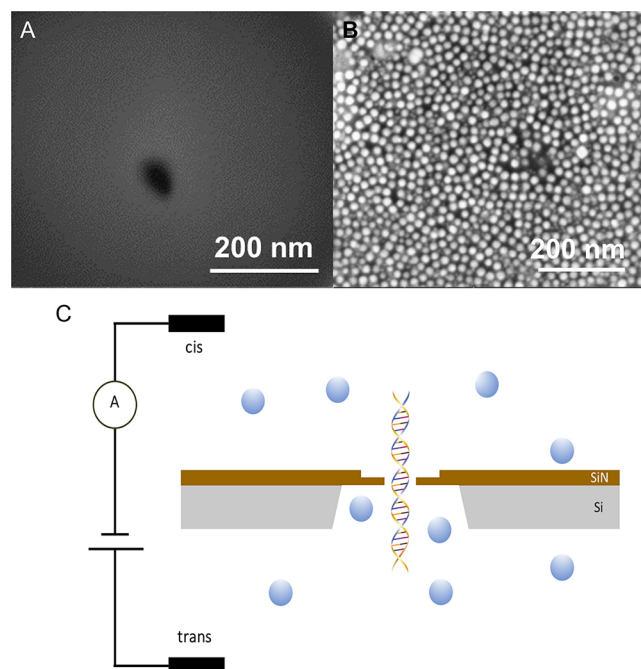


Figure 1. (A) SEM image of a SiN nanopore with a diameter of 45 nm; (B) SEM image of NPs with a diameter of about 20 nm; (C) scheme of a nanopore sensor detecting a DNA molecule translocating through the nanopore.

microscopy (SEM) image of the nanopore. In the meantime, a patch-clamp amplifier system (EPC10, HEKA Elektronik) was used to establish a platform for detecting the ion current in order to accurately detect the small current changes caused by molecules translocating through the nanopore.

The nanopore sensor was initially evaluated by measuring the ionic current, and its ionic conductivity was characterized. The amplitude of the ionic current blockage is the difference between the ionic current through the nanopore in the open state (I_{open}) and that in the blocked state (I_{blocked}), expressed as $\Delta I = I_{\text{open}} - I_{\text{blocked}}$. The patch clamp amplifier can be used to

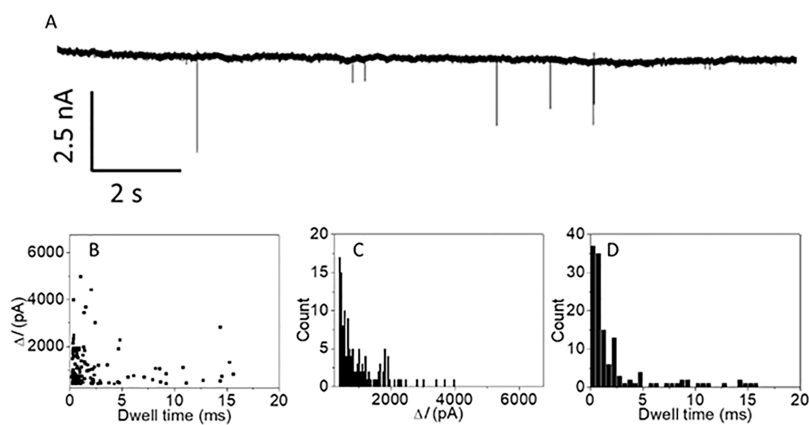


Figure 2. (A) Ionic current diagram for detection of NPs; (B) scatter diagram of the ionic current through nanopores; (C) amplitude distribution of the current blockade during the sample translocation through the nanopore; (D) dwell time distribution of the current histogram of the current blockade during the sample translocation through the nanopore.

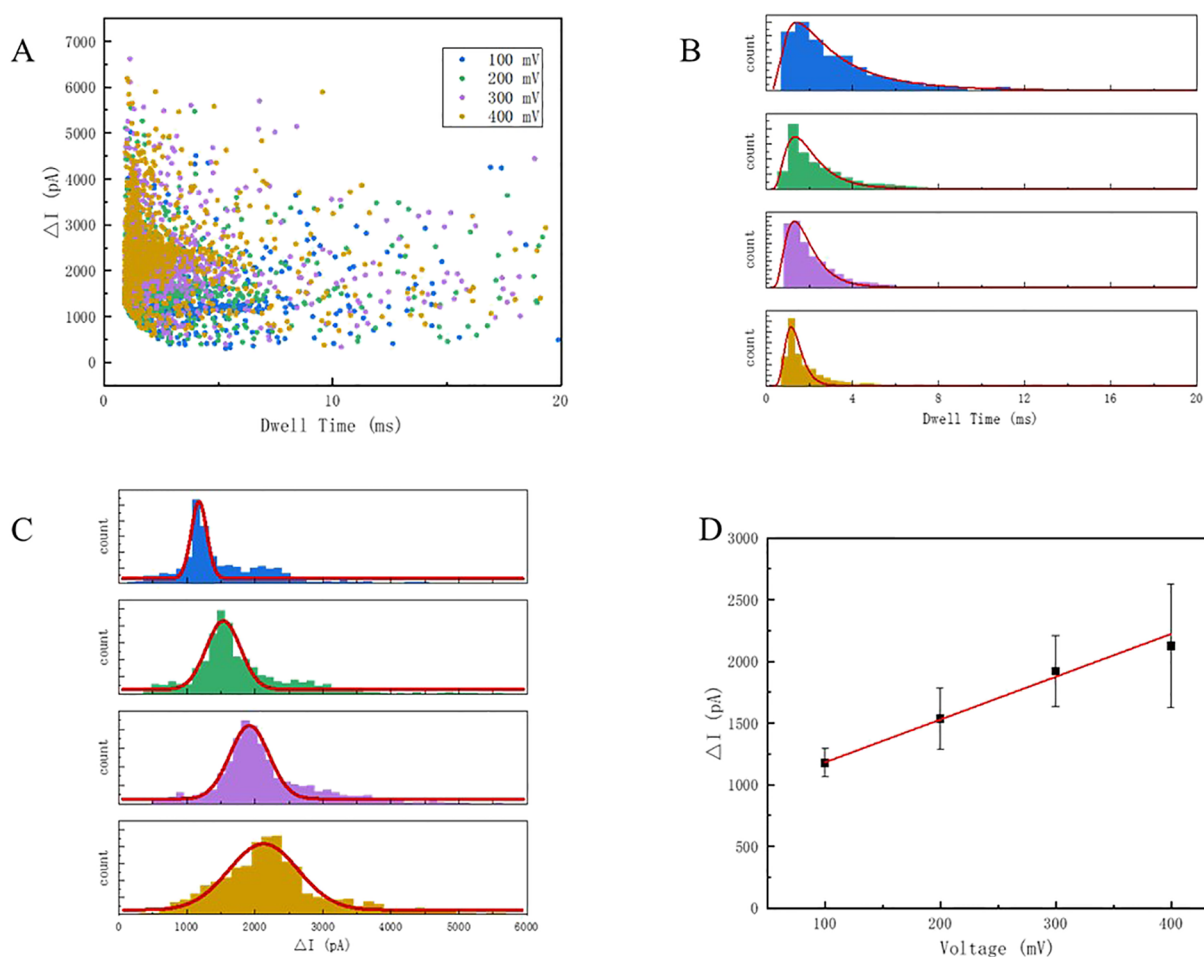


Figure 3. NP translocation events through the nanopore. (A) Scatter diagram of ionic current in the bias voltage range of 100–400 mV; (B) histograms of dwell time under different bias voltages; and (C) amplitude distribution histogram of NP samples under different bias voltages. (D) Mean amplitude of ionic pulses.

apply different bias voltages at both ends of an ion solution-filled nanopore and to measure the corresponding ionic current value to obtain the corresponding current–voltage curve (I – V curve). According to the formula $G = I/V$, the ionic conductivity of the nanopore is the slope of the linear fitting of the I – V curve.

2.2. Preparation of NPs. Spherical silver NPs with a diameter of 20 nm were synthesized in this experiment. First, in 20 mL of an aqueous solution of K_2PdCl_4 (1 mM) or $AgNO_3$ (1 mM) containing poly (*N*-vinyl-2-pyrrolidone) (PVP) (0.5 wt %) or 3,3'-thiodipropionic acid (TDPC) (1 mM), 0.028 g of potassium hydroxide (KOH) was dissolved. Then, the solution was added to 20 mL of aqueous potassium

bitartrate (0.5 wt %) solution that was stirred and heated to approximately 100 °C. After 2 h of continuous reflux with agitation, palladium colloid was produced, and the solution turned dark brown or green, indicating the formation of silver NPs. It was also confirmed by additional SEM characterization (Figure 1B).

The average size of NPs was determined by randomly selecting over 2000 NPs from SEM images. Before subsequent experiments, the nanoparticle containing solution was also subjected to ultrasonic oscillations, ensuring that the NPs were evenly dispersed and preventing aggregation.

2.3. Preparation of DNA-Modified Nanoparticles. This experiment utilized streptavidin-coated silver NPs with a diameter of 20 nm (Zhongkekeyou, China) to prepare DNA/particle constructs. Streptavidin-coated nanoparticle suspension (5 mL) was used to bind 5 mL of biotinylated λ -DNA (48.5 kb) at a concentration of 1 nM. The DNA primers were acquired in Sangon, China. To wash the beads, 100 mL of buffer (100 mM KCl, 10 mM Tris-EDTA) was added to a 1.5 mL centrifuge tube containing beads. After spinning down the beads with a laboratory centrifuge and removing the supernatant with a pipette, the washing step was repeated. Next, the beads were resuspended in 5 mL of binding buffer (2 M KCl, 10 mM Tris-EDTA), DNA at a concentration of 1 nM in 10 mM Tris-EDTA buffer was added, and the sample was incubated for 15 min at room temperature. After repeating the washing step, the DNA/particle constructs were resuspended to the desired concentration in the measurement buffer.

3. RESULTS

3.1. Nanoparticle Detection Based on Nanopores.

The NPs were detected using a 45 nm SiN nanopore. KCl (1 M) was used as the electrolyte solution, and the pH value of the electrolyte solution was adjusted to 8.0 using 10 mM Tris-HCl and 1 mM EDTA buffer. Before the experiment, NPs were added into the cis chamber (chamber with cathode). The process of NPs translocating through the nanopore driven by bias voltage can be successfully detected, as shown in Figure 2A. The scatter diagram of ionic current pulses is shown in Figure 2B. The distributions of ionic current amplitude distribution and dwell time distribution of the sample passing through a nanopore were calculated using histograms (Figure 2C, D). It can be seen that the current blockade of the sample translocating through the nanopore can be distinguished clearly from the background noise.

Then, NP detection experiments were conducted using various bias voltages. The ionic current signals of NP translocation events were detected and analyzed (Figure 3A–D). In the range of 100–400 mV bias voltage, the duration time of the translocation events decreases as the voltage becomes higher. Meanwhile, the amplitude of the current blockades is proportional to the magnitude of bias voltage. It clearly shows that ΔI increases linearly with the increase of bias voltage, demonstrating once again that the translocation of NPs causes the resistive pulse ionic current through the nanopore.

3.2. DNA Molecular Detection Based on Nanopores.

This experiment is designed to distinguish between NPs and DNA molecules using a nanopore sensor to validate further the viability of a nanopore sensor for single-molecule detection. As shown in Figure 4A, the diameter of SiN nanopores is 30 nm. The λ -DNA molecules with a length of 48.5 kbp were used in this experiment.

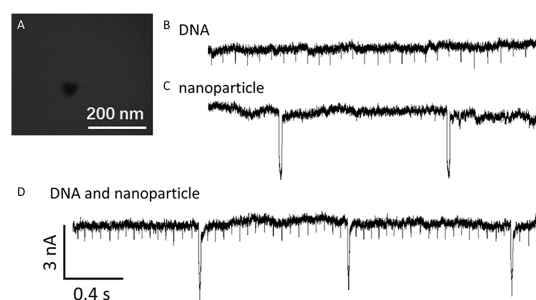


Figure 4. (A) SEM image of SiN nanopores with a diameter of 30 nm; (B) ionic current trace for detection of DNA; (C) ionic current trace for detection of NPs; and (D) ionic current trace for detection of NPs and DNA mixed samples.

When the nanopore is used to detect DNA, NPs, and their mixed samples, the corresponding current trace diagram, as shown in Figure 4B–D, will be captured.

Due to the physical occupying effect, changes in ionic conductivity should decrease as analytes translocate through nanopores. According to the volume occupied by DNA, the amplitude change of ionic conductance should be

$$\Delta G = G_{\text{open pore}} - G_{\text{with molecule}} = G(d) - G(d_{\text{with molecule}}) \quad (1)$$

$$\text{In eq 1, } d_{\text{with molecule}} = \sqrt{d^2 - d_{\text{molecule}}^2}$$

$$G(d) = \left(\frac{4h}{\pi d^2} + \frac{1}{d} \right)^{-1} [(n_+ \mu_+ + n_- \mu_-) e]$$

In formula 1, d – the diameter of the nanopore; d_{molecule} – the diameter of the molecule to be measured; h – the length of the nanopore; n_+ – the quantitative density of the positive ions; n_- – the quantitative density of the negative ions; μ_+ – electrophoretic mobility of the positive ions; μ_- – electrophoretic mobility of the negative ions; e – elementary charge.

When only DNA was present, statistical analysis revealed that the amplitude of the current signals was 670 pA. The double-stranded DNA molecule diameter is 2.2 nm, and the corresponding blocking current can be calculated using formula 1. Moreover, the calculated result (667 pA) corresponds to the experimental outcome (Figure 5A–C).

The dwell time of DNA molecules in most translocation events described in this study is approximately 2 ms, which is comparable to previous research findings. Some translocation events with longer dwell time may be caused by the interactions between DNA molecules and nanopore walls. In this study, the likelihood of such a long-term event occurring is extremely low, consistent with previous research. The scatter diagram displays two distinct peaks when DNA molecules and NPs are present in the detected samples (Figure 5D–F). Given that, the diameter of DNA molecules is significantly smaller than that of NPs, and the amplitude of the DNA-induced blocking current is also significantly smaller than that of NPs. Two prominent peaks can also be observed on the current signal's histogram. Thus, the nanopore with a diameter of 30 nm can effectively distinguish between the events of DNA molecules and NPs translocating through the nanopore. However, it is also important to note that although DNA molecules are significantly longer than NPs, its translocation time is smaller than NPs.

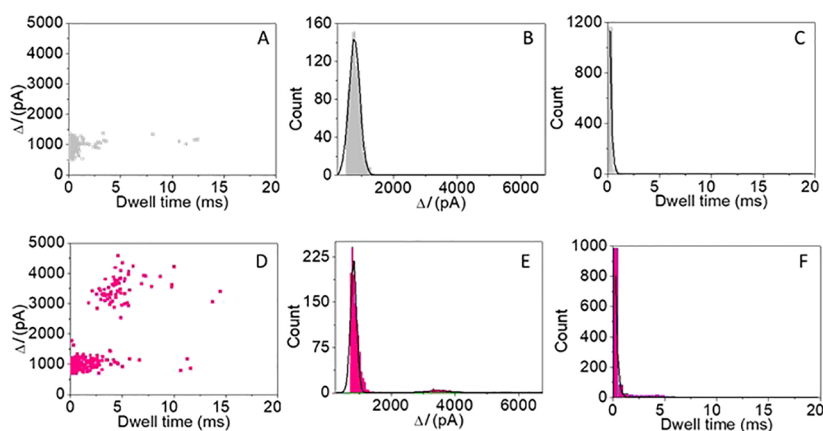


Figure 5. (A–C) DNA translocation through the nanopore. (A) Scatter diagram of ionic current; (B) amplitude distribution histogram of ionic current; (C) histogram of translocation time distribution; (D–F) mixed samples of NPs and DNA translocation through the nanopore. D. Scatter diagram of ionic current; E. amplitude distribution histogram of ionic current; F. histogram of translocation time distribution

3.3. DNA-Modified NP Detection Based on Nanopores.

In order to further demonstrate the viability of large-diameter nanopore sensors for DNA detection, we supplemented our previous experiments to identify NP-bound DNA molecules using nanopore sensors. In this experiment, probes were modified to bind the target DNA to silver NPs. We used a 53 nm diameter nanopore to detect free DNA molecules and DNA-particle conjugated samples. As shown in Figure 6, the

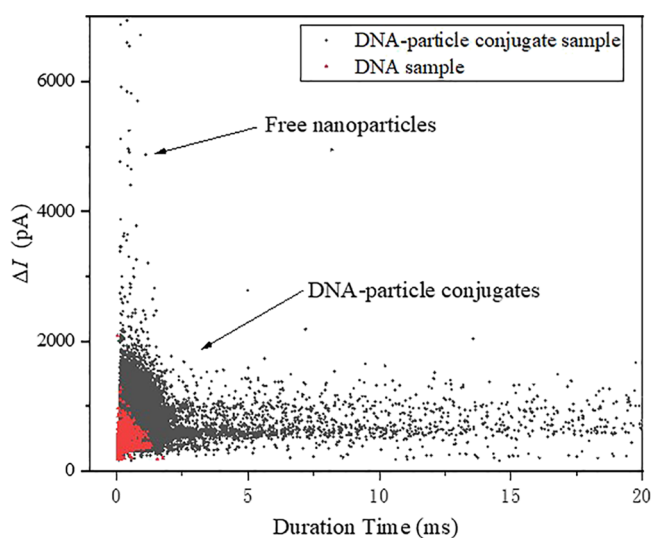


Figure 6. Scatter diagram of translocation ionic current of DNA-particle conjugated samples and free DNA molecule samples detected by the nanopore sensor.

red scatters represent the free DNA translocation events, whereas the black scatters represent DNA-particle conjugated sample translocation events. It clearly shows DNA-particle conjugates cause a larger blocking current than free nontarget DNA molecules when they passed through the nanopore. However, the amplitude of such ionic currents is smaller than that caused by the translocation events of NPs alone. This is because the surface charge of DNA is stronger than silver NPs. Driven by electric field force, DNA-particle conjugates pass through the nanopore with a velocity $\sim 10 \mu\text{m}/\text{ms}$, which is much faster than NPs passing through the nanopore alone. The diameter of silver NPs is only about 20 nm, and the

residence time of silver NPs traversing the nanopore pulled by DNA is only $2 \mu\text{s}$. The current traces were measured at 200 kHz with a 10 kHz low-pass filter due to the sensitivity limits of the patch clamp amplifier. Therefore, the ionic pulse is hard to reflect the structure of NPs from DNA-particle conjugate translocation events. Nevertheless, streptavidin-coated silver NPs can simultaneously bind to multiple probes and target DNA molecules. The length of the target DNA molecule (48.5 kbp) is about $16.5 \mu\text{m}$. It indicates that the ionic pulses of DNA-particle conjugates were generated by the translocation process of multiple DNA molecules rather than the NPs. Here, the streptavidin-coated silver NPs only play a role of a link among multiple target DNA. With the assistance of NPs, nanopore sensors are able to identify the target DNA according to the ionic pulse signals.

4. DISCUSSION

In this study, SiN nanopore sensors were used to detect DNA molecules and silver NPs separately and in combination. Like this study, Mereuta et al. investigated DNA hybridization probes immobilized on the surface of gold NPs for the sequence-specific detection of short-length nucleic acids by large-size (tip diameter of 20 nm) nanopore sensors.^{17,19} It proved that it is feasible to detect target nucleic acid molecules using large diameter nanopores assisted by NPs. However, the critical issue in implementing nanoparticle-assisted nanopore sensors to detect target DNA is the need to be able to distinguish free DNA, NPs, and DNA-bound-NPs according to the amplitude of the translocation current.

This study demonstrated that the amplitude of the translocation current of the free DNA molecule is the lowest since it has a small diameter, whereas the nanoparticle has a large diameter and the amplitude of the current is relatively large. Because DNA-modified NPs were bound to multiple DNA molecules, the translocation speed of the conjugates as a whole is fast, and the generated current signal cannot reflect the structure of NPs. Since multiple DNA molecules in the conjugates passed through the nanopore at the same time, the current amplitude is larger than that of the free DNA molecule and smaller than that of the free NPs. Accordingly, the DNA-modified NPs can be distinguished from the free DNA and the free NPs.

On the other hand, Mereuta et al. used protein bio-nanopores, the preparation and detection of which required a

specific experimental and detection environment.¹⁸ Moreover, poor nanopore stability can result in a lack of detection stability of the detection. In our research, NPs and DNA molecules are successfully detected and distinguished using solid nanopores, which is anticipated to increase the detection sensitivity of nanopore sensors in various experimental settings.

However, there are still some limitations that require further investigation. For instance, solid-state nanopore sensors may be utilized for more precise detection and analysis, such as nucleotide identification of DNA molecules bound to NPs, to meet the demand of high-resolution detection of target molecules and rapid sequencing scenarios.

5. CONCLUSIONS

In conclusion, our research indicates that large-sized nanopores can distinguish between the translocation events of DNA, NPs, and nanoparticle-bound DNA molecules based on the amplitude and duration of the ionic current, thereby identifying the presence of the target DNA molecules in the sample. This nanopore-sensing platform can produce rapid and accurate nucleic acid detection. Its application in medical diagnosis, gene therapy, virus identification, and many other fields is highly significant.

AUTHOR INFORMATION

Corresponding Author

Yang Shen – Department of Obstetrics and Gynecology, School of Medicine, Zhongda Hospital, Southeast University, Nanjing, Jiangsu 210009, China; orcid.org/0000-0002-3313-5062; Phone: 0086-025-83262742; Email: shenyang@seu.edu.cn

Authors

Bo Ding – Department of Obstetrics and Gynecology, School of Medicine, Zhongda Hospital, Southeast University, Nanjing, Jiangsu 210009, China

Xin-Yi Hong – Department of Obstetrics and Gynecology, School of Medicine, Southeast University, Nanjing, Jiangsu 210009, China; orcid.org/0000-0002-1386-6474

Han Yin – Department of Obstetrics and Gynecology, School of Medicine, Southeast University, Nanjing, Jiangsu 210009, China

Jing-Yun Xu – Department of Obstetrics and Gynecology, School of Medicine, Zhongda Hospital, Southeast University, Nanjing, Jiangsu 210009, China

Xiao-Yu Zhang – Department of Obstetrics and Gynecology, School of Medicine, Zhongda Hospital, Southeast University, Nanjing, Jiangsu 210009, China

Qing Zhou – Department of Obstetrics and Gynecology, School of Medicine, Southeast University, Nanjing, Jiangsu 210009, China

Complete contact information is available at: <https://pubs.acs.org/10.1021/acsomega.3c00152>

Author Contributions

[§]B.D. and X.-Y.H. contributed to the work equally and should be regarded as co-first authors. Conceptualization, Y.S.; methodology, B.D.; formal analysis, X.-Y.H.; software, H.Y.; validation, X.-Y.H. and Q.Z.; investigation, J.-Y.X.; writing—original draft preparation, X.-Y.H. All authors have read and agreed to the published version of the manuscript.

Funding

This research was funded by the Scientific Research Project of Jiangsu Health Commission (ZDA2020012), Jiangsu Provincial Key Research and Development Program (SBE2020741118), and Postgraduate Research & Practice Innovation Program of Jiangsu Province (SJCX21-0081).

Notes

The authors declare no competing financial interest.

ACKNOWLEDGMENTS

We hereby express our thanks to Professor Yin Zhang and his team from the School of Mechanical Engineering of Southeast University for the guidance and support for this study.

REFERENCES

- (1) Dekker, C. Solid-state nanopores. *Nat. Nanotechnol.* **2007**, *2*, 209–215.
- (2) Branton, D.; Deamer, D. W.; Marziali, A.; Bayley, H.; Benner, S. A.; Butler, T.; Di Ventra, M.; Garaj, S.; Hibbs, A.; Huang, X.; et al. The potential and challenges of nanopore sequencing. *Nat. Biotechnol.* **2008**, *26*, 1146–1153.
- (3) Kumar, H.; Lansac, Y.; Glaser, M. A.; Maiti, P. K. Biopolymers in nanopores: challenges and opportunities. *Soft Matter* **2011**, *7*, 5898–5907.
- (4) Venkatesan, B. M.; Bashir, R. Nanopore sensors for nucleic acid analysis. *Nat. Nanotechnol.* **2011**, *6*, 615–624.
- (5) Li, W.; Bell, N. A. W.; Hernandez-Ainsa, S.; Thacker, V. V.; Thackray, A. M.; Bujdoso, R.; Keyser, U. F. Single Protein Molecule Detection by Glass Nanopores. *ACS Nano* **2013**, *7*, 4129–4134.
- (6) Steinbock, L. J.; Stober, G.; Keyser, U. F. Sensing DNA-coatings of microparticles using micropipettes. *Biosens. Bioelectron.* **2009**, *24*, 2423–2427.
- (7) Roberts, G. S.; Kozak, D.; Anderson, W.; Broom, M. F.; Vogel, R.; Trau, M. Tunable Nano/Micropores for Particle Detection and Discrimination: Scanning Ion Occlusion Spectroscopy. *Small* **2010**, *6*, 2653–2658.
- (8) Balagurusamy, V. S. K.; Weinger, P.; Ling, X. S. Detection of DNA hybridizations using solid-state nanopores. *Nanotechnology* **2010**, *21*, No. 335102.
- (9) Peng, H.; Ling, X. S. Reverse DNA translocation through a solid-state nanopore by magnetic tweezers. *Nanotechnology* **2009**, *20*, No. 185101.
- (10) Booth, M. A.; Vogel, R.; Curran, J. M.; Harbison, S.; Travas-Sejdic, J. Detection of target-probe oligonucleotide hybridization using synthetic nanopore resistive pulse sensing. *Biosens. Bioelectron.* **2013**, *45*, 136–140.
- (11) Esfandiari, L.; Lorenzini, M.; Kocharyan, G.; Monbouquette, H. G.; Schmidt, J. J. Sequence-Specific DNA Detection at 10 fM by Electromechanical Signal Transduction. *Anal. Chem.* **2014**, *86*, 9638–9643.
- (12) Esfandiari, L.; Monbouquette, H. G.; Schmidt, J. J. Sequence-specific Nucleic Acid Detection from Binary Pore Conductance Measurement. *J. Am. Chem. Soc.* **2012**, *134*, 15880–15886.
- (13) Zhang, Y. Q.; Rana, A.; Stratton, Y.; Czyzyk-Krzeska, M. F.; Esfandiari, L. Sequence-Specific Detection of MicroRNAs Related to Clear Cell Renal Cell Carcinoma at fM Concentration by an Electroosmotically Driven Nanopore-Based Device. *Anal. Chem.* **2017**, *89*, 9201–9208.
- (14) Koo, B.; Yorita, A. M.; Schmidt, J. J.; Monbouquette, H. G. Amplification-free, sequence-specific 16S rRNA detection at 1 aM. *Lab Chip* **2018**, *18*, 2291–2299.
- (15) Joung, H.-A.; Lee, N.-R.; Lee, S. K.; Ahn, J.; Shin, Y. B.; Choi, H.-S.; Lee, C.-S.; Kim, S.; Kim, M.-G. High sensitivity detection of 16S rRNA using peptide nucleic acid probes and a surface plasmon resonance biosensor. *Anal. Chim. Acta* **2008**, *630*, 168–173.
- (16) Roy, S.; Zanolli, K. J.; Murphy, C. T.; Tanius, F. A.; Wilson, W. D.; Ly, D. H.; Armitage, B. A. Kinetic discrimination in

recognition of DNA quadruplex targets by guanine-rich heteroquadruplex-forming PNA probes. *Chem. Commun.* **2011**, *47*, 8524–8526.

(17) Zhang, Y.; Chen, X.; Wang, C.; Chang, H.-C.; Guan, X. Nanoparticle-assisted detection of nucleic acids in a polymeric nanopore with a large pore size. *Biosens. Bioelectron.* **2022**, *196*, No. 113697.

(18) Mereuta, L.; Asandei, A.; Dragomir, I. S.; Bucataru, I. C.; Park, J.; Seo, C. H.; Park, Y.; Luchian, T. Sequence-specific detection of single-stranded DNA with a gold nanoparticle-protein nanopore approach. *Sci. Rep.* **2020**, *10*, 11323.

(19) Ang, Y. S.; Yung, L.-Y. L. Rapid and Label-Free Single-Nucleotide Discrimination via an Integrative Nanoparticle-Nanopore Approach. *ACS Nano* **2012**, *6*, 8815–8823.